Available online at www.sciencedirect.com
ScienceDirect
Applied Catalysis A: General 325 (2007) 276–282
APPLIED CATALYSIS A: GENERAL
www.elsevier.com/locate/apcata

Photo-oxidation of ethanol on mesoporous vanadium–titanium oxide catalysts and the relation to vanadium(IV) and (V) sites

Dilshad Masih [a], Hideaki Yoshitake [b], Yasuo Izumi [a,*]

[a] *Interdisciplinary Graduate School of Science and Engineering, Tokyo Institute of Technology, Nagatsuta 4259-G1-16, Midori-ku, Yokohama 226-8502, Japan*

[b] *Graduate School of Environment and Information Sciences, Yokohama National University, Tokiwadai, Hodogaya-ku, Yokohama 240-8501, Japan*

Received 21 July 2006; accepted 7 February 2007
Available online 3 March 2007

Abstract

Ethanol photo-oxidation was investigated over mesoporous, amorphous V + TiO_2 and V + TiO_2(anatase) catalysts. Under the UV + visible light, mesoporous V + TiO_2 generally exhibited faster photo-oxidation rates than V + TiO_2(anatase) catalysts did. V^{IV} doping directed preferable formation of acetic acid rather than predominant acetaldehyde formation. Under the visible light only, mesoporous V^{IV}–TiO_2 catalyst exhibited best reactivity among all V + TiO_2 catalysts. Ethanol dehydration reaction was preferred. Initial quicker water evolution may suggest greater oxidation capability compared to V + TiO_2(anatase) catalysts.

Keywords: Photocatalyst; Photocatalysis; Oxidation; Vanadium; Titania; Mesoporous; UV–vis

1. Introduction

Titanium dioxide works as photocatalysts based on the semiconducting property [1,2]. The light absorption by TiO_2 predominantly lies in UV range. Only 3% of solar energy is utilized using the anatase TiO_2 phase at the surface of earth [1]. The modification of TiO_2 improved the efficiency of solar radiation utilization up to 20–30% by adding different elements, *e.g.* chromium, vanadium, platinum, or nitrogen to TiO_2 [3–9]. In contrast, chloride, sulfate, or phosphate exhibited detrimental effects on the photocatalysis [10–13].

To improve the photocatalysis of TiO_2-based materials, another approach is to synthesize mesoporous TiO_2 with high specific surface area. The applications of nano-crystalline and mesoporous TiO_2 to the photodecomposition of 2,4,6-trichloropheonol and other organic compounds were suggested utilizing the availability of larger number of active sites [14,15]. Syntheses of mesoporous and nano-crystalline TiO_2 were reported via different routes [15–22]. In this paper, wormhole-like, amorphous mesoporous materials with specific surface area as much as 1200 $m^2\ g^{-1}$ were used [23,24]. The doping effect on the red shift of UV–vis absorption was reported to follow the order V > Cr > Mn > Fe > Ni to TiO_2 [3]. Therefore, series of mesoporous V + TiO_2 samples were prepared and the performance of ethanol photo-oxidation reaction was compared to conventional V + TiO_2(anatase) catalysts with the illumination of UV + visible light or visible light only.

The V site structures on/in TiO_2 have been intensively studied by means of Raman, UV–vis, ^{51}V nuclear magnetic resonance, and X-ray absorption fine structure spectroscopies [25–28] and we recently reported the V structure transformation in on-site conditions and also the V structure for mesoporous V + TiO_2 catalysts [24,29]. The ethanol photo-oxidation reactivity over various mesoporous and conventional V + TiO_2 catalysts was compared to the V site structure (geometric and electronic) information.

2. Experimental

2.1. Syntheses of V + TiO_2 catalysts

TiO_2 (P-25, Degussa) with a specific surface area of 60 $m^2\ g^{-1}$ was impregnated with V triisopropoxide oxide (**1**) in

* Corresponding author. Tel.: +81 45 924 5569; fax: +81 45 924 5569.
E-mail address: izumi.y.ac@m.titech.ac.jp (Y. Izumi).

0926-860X/$ – see front matter
doi:10.1016/j.apcata.2007.02.037

2-propanol solution (impregnated V/TiO_2). Major phase of TiO_2 (P-25) was anatase being the ratio of anatase/rutile 95/5. Mesoporous V–TiO_2 samples were prepared from compound **1**, Ti tetraisopropoxide (**2**), and dodecylamine (**3**). An aqueous solution of the reactants was maintained at 333 K for 6 days and then filtered. The obtained powder was heated at 453 K for 10 days, and then washed with *p*-toluenesulfonic acid in ethanol. Based on X-ray diffraction patterns, the basal spacing was 30 Å and a wormhole-like structure prevailed rather than highly ordered periodic mesostructure [23,24]. Following similar route, mesoporous TiO_2 was synthesized from compounds **2** and **3**. Mesoporous TiO_2 was impregnated with compound **1** in 2-propanol (V/mesoporous TiO_2). The V contents in these samples were 3.0 or 1.0 wt% on the V metal basis. All the dried powders were calcined in air at 523 K.

2.2. Ethanol photo-oxidation measurements on V + TiO_2 catalysts

The reaction was performed in a closed circulating glass system (total volume 132 ml). Hundred milligrams of catalyst was homogeneously spread in a quartz reaction cell (bottom plate area 23.8 cm^2) and illuminated with UV–vis light from xenon arc lamp operated at 500 W (UXL-500D, Ushio). The catalyst was set at 2 mm apart from the exit window of the light. The distance between catalyst and the mirror set in the light path was 65 mm. Kenko UV-cut filter L-42 was set on the light exit window for photocatalysis measurements under visible light only.

Before the photo-oxidation reaction measurements, all the catalysts were evacuated (10^{-6} Pa) for 2 h at 290 K. Photocatalytic oxidation of 55 μmol of gas phase ethanol was carried out at 290 K [30–34]. One hundred and ten micromoles of oxygen was introduced as an oxidant [30]. Products and reactants were analyzed using online gas chromatograph equipped with thermal conductivity detector (Shimazu GC-8A) connected to the closed circulating system. All the reaction products and reactants were analyzed using Porapak-Q column (GL Sciences).

2.3. UV–vis absorption spectrum measurements for V + TiO_2 catalysts

Optical spectra were recorded on UV–vis spectrometer V-550 (Jasco) equipped with an integrating sphere attachment ISV-470 (Jasco) for diffuse-reflectance measurements. Measurements were made at 290 K in the wavelength range between 280 and 650 nm. UV–vis absorbance for all the compounds was obtained by the transformation based on the Kubelka–Munk equation.

3. Results

3.1. Ethanol photo-oxidation kinetics with UV–vis illumination

The time course of photo-oxidation reaction for ethanol (initial pressure 1.33 kPa) was depicted in Fig. 1 on mesoporous V + TiO_2 catalysts. Major products were acetaldehyde, water, carbon dioxide, and acetic acid on mesoporous TiO_2 (Fig. 1A) [34]. Because the ratio of formation rates for acetaldehyde and water was 2.2 (Table 1A), dehydration and dehydrogenation reactions for ethanol proceeded with comparable rates. Further photo-oxidized products acetic acid and carbon dioxide were minor. The formations of ethene and carbon monoxide were negligible.

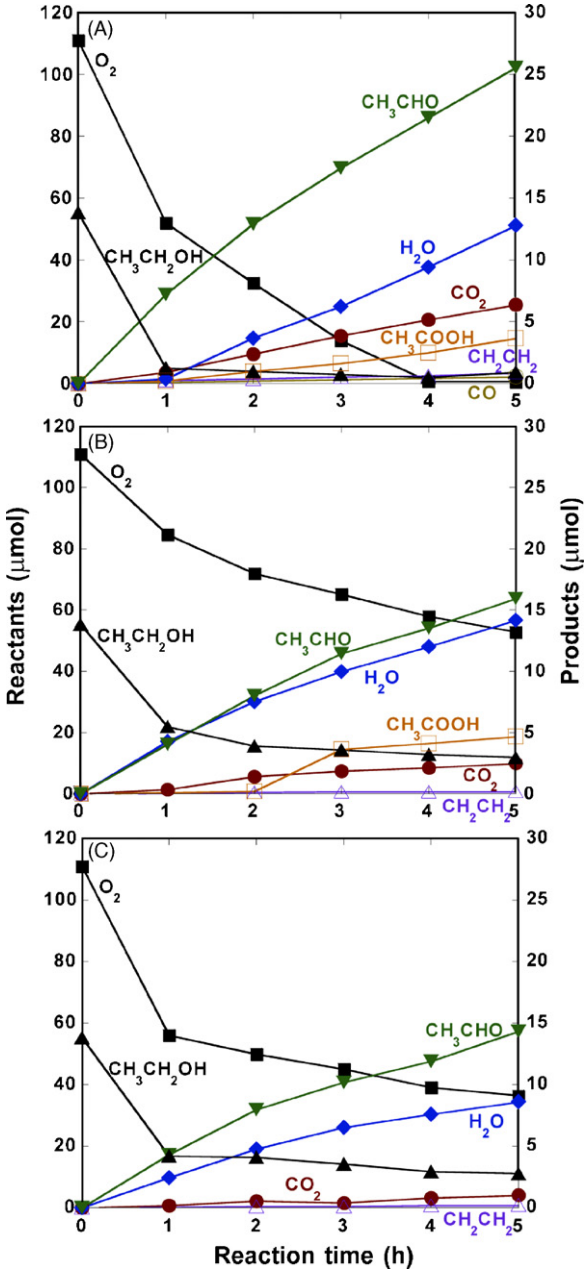

Fig. 1. Ethanol oxidation reaction as a function of time under the illumination of UV–vis light on mesoporous V + TiO_2 catalysts. Measured at 290 K. Ethanol (1.33 kPa) and O_2 (2.67 kPa) were introduced in closed circulating glass system (132 ml). (A) Mesoporous TiO_2. (B) Mesoporous V–TiO_2 (3.0 wt% V). (C) Impregnated V/mesoporous TiO_2 (3.0 wt% V).

In the photo-oxidation over mesoporous V–TiO_2 (3.0 wt% V), acetaldehyde and water were produced with essentially the same rates (Fig. 1B). Thus, ethanol dehydration proceeded predominantly in the presence of vanadium in the TiO_2 matrix [29]. Acetic

Table 1
Products formation rates in the ethanol photo-oxidation over various V + TiO_2 catalysts illuminated with UV + visible light (A) and visible light only (B)[a]

	Formation rates (μmol h^{-1} g_{cat}^{-1})						
	MeCHO	H_2O	$MeCO_2H$	CO	CO_2	C_2H_4	Σ^f
(A) UV + visible							
Mesoporous TiO_2	72	33[c]	11[c]	0.85	14[c]	1.3	92
Mesoporous V–TiO_2[b]	42	44	35[c]	0	8.8[c]	0.2	82
V/mesoporous TiO_2[b]	43	24	0	0	2.1[c]	0.3	44
TiO_2 (P-25)	61	50[d]	0	0.3	6.4	0	64
V/TiO_2[b]	28	0	0	0	0.1	0	28
(B) Visible only							
Mesoporous TiO_2	2.3	16[c]	0	0	0.3[c]	0	2.5
Mesoporous V–TiO_2[b]	23	212(16[e])	0	0	0.3[c]	0	23
V/mesoporous TiO_2[b]	11	141(15[e])	0	0	0.2[c]	0	11
TiO_2 (P-25)	19	4.9[c]	0	0	0.2[c]	0	19
V/TiO_2[b]	18	0	0	0	0.9[c]	0	18

[a] Initial reactants: CH_3CH_2OH (55 μmol) and O_2 (110 μmol).
[b] 3.0 wt% V.
[c] Constant rates later than the induction period.
[d] Serious deactivation observed.
[e] Constant rate later than initial faster rate.
[f] The summation of formation rates on the basis of carbon. The formation rates of CO and CO_2 were multiplied with a half in the summation.

acid and carbon dioxide produced later than the induction period of 1–2 h because they were secondary or multiple-step products. For the impregnated V/mesoporous TiO_2 catalyst, the ratio of acetaldehyde and water formation rates was 1.8 (Fig. 1C and Table 1A). Thus, ethanol dehydration and dehydrogenation reactions proceeded with the rate ratio 1.3. Minor products were carbon dioxide and ethene. Compared to reactions on mesoporous TiO_2 and mesoporous V–TiO_2 (Fig. 1A and B), no acetic acid was found over impregnated V/mesoporous TiO_2.

The kinetics of ethanol photo-oxidation on V + TiO_2 (P-25) catalysts were summarized in Fig. 2 and Table 1A. On TiO_2 (P-25), major products were acetaldehyde and water, however, the formation rates were not constant (Fig. 2A) compared to the kinetics on mesoporous V + TiO_2 catalysts. The time course change for water formation was not monotonous. It was first deactivated and reactivated at 3 h. When vanadium was impregnated on TiO_2 (P-25) (Fig. 2B), the catalysis was suppressed compared to pure TiO_2 (P-25). Acetaldehyde was essentially the only one product via the ethanol dehydrogenation. The ethanol amount even increased in first 1 h in Fig. 2B. On vanadium-doped TiO_2 formic acid formation was reported [34], and in our Porapak-Q column formic acid and ethanol were not separated. Thus, the initial apparent increase of ethanol may be catalytic formation of formic acid.

In summary, under the illumination of UV–vis light, the ethanol dehydration rates followed the order (Table 1A)

$$TiO_2 \approx \text{mesoporous V}-TiO_2 > \text{mesoporous } TiO_2 > \text{V/mesoporous } TiO_2 \gg \text{V/}TiO_2 \quad (1)$$

Ethanol dehydrogenation rates assumed based on the difference of acetaldehyde and water formation rates followed the order

$$\text{mesoporous } TiO_2 > \text{V/}TiO_2 > \text{V/mesoporous } TiO_2 > TiO_2 \gg \text{mesoporous V}-TiO_2 \quad (2)$$

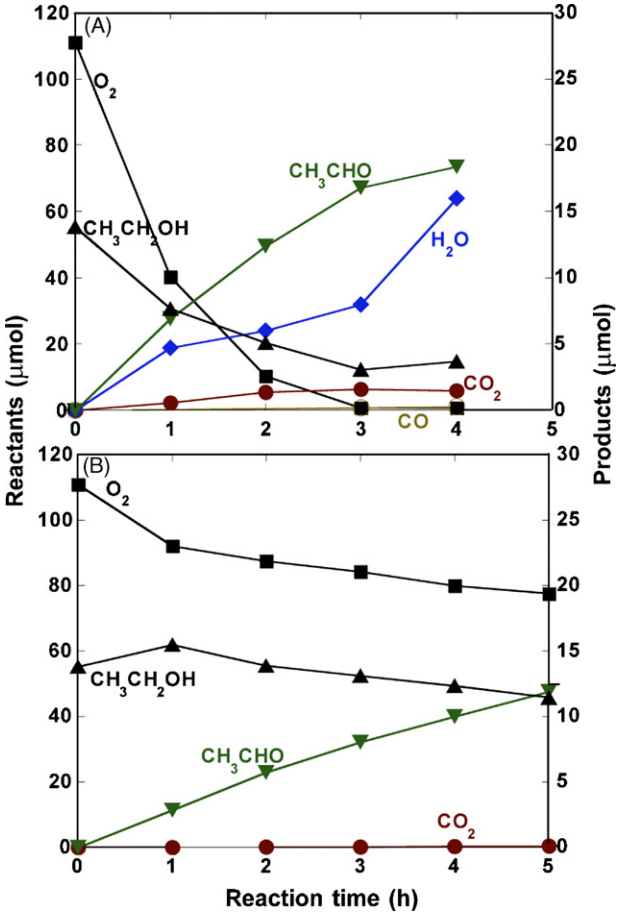

Fig. 2. Ethanol oxidation reaction as a function of time under the illumination of UV–vis light on conventional V + TiO_2 (P-25) catalysts. Reaction conditions were the same as noted in the caption for Fig. 1. (A) TiO_2 (P-25). (B) Impregnated V/TiO_2 (3.0 wt% V).

Acetic acid (and carbon dioxide) formation rates followed the order

$$\text{mesoporous V}-\text{TiO}_2 > \text{mesoporous TiO}_2 \gg \text{V/mesoporous TiO}_2 \approx \text{TiO}_2 \approx \text{V/TiO}_2 \quad (3)$$

Ethanol photo-oxidation was reported on anatase TiO_2 and platinum-modified one [7]. The addition of Pt enabled catalytic formation of acetic acid similar to over mesoporous [V–]TiO_2 (Table 1A).

3.2. Ethanol photo-oxidation kinetics with visible light only illumination

The ethanol photo-oxidation results on mesoporous V + TiO_2 with visible light only illumination were depicted in Fig. 3 and the formation rates were summarized in Table 1B. The mesoporous TiO_2 catalyst was fairly inactive compared to the case illuminated with UV + visible light (Figs. 3A and 1A). Water was formed in addition to negligible acetaldehyde and carbon dioxide. Because the water evolving rate was greater than that of acetaldehyde by 7.0 times and ethanol in gas phase significantly decreased in the first 1 h, formed acetaldehyde may be trapped in mesopores of the TiO_2.

For mesoporous V–TiO_2 catalyst (3.0 wt% V), water was formed in first 1 h faster than for mesoporous TiO_2 by 13 times (Fig. 3B), even faster than in the measurement with UV + visible light illumination (Fig. 1B) by 4.8 times. Later than 1 h, the formation rates of water and acetaldehyde became constant and comparable (16 and 23 $\mu mol\ h^{-1}\ g_{cat}{}^{-1}$, respectively, Table 1B). Minor product was carbon dioxide. The kinetic result for impregnated V/mesoporous TiO_2 (Fig. 3C) was qualitatively similar to that for mesoporous V–TiO_2 (Fig. 3B). Initial faster evolution of water was again observed in first 1 h and then water and acetaldehyde were constantly produced (15 and 11 $\mu mol\ h^{-1}\ g_{cat}{}^{-1}$, respectively). The constant formation rates decreased to 94 and 48%, respectively, of corresponding rates for mesoporous V–TiO_2 (Table 1B).

Illuminated with visible light only, ethanol dehydrogenation proceeded predominantly at the rate between 18 and 19 $\mu mol\ h^{-1}\ g_{cat}{}^{-1}$ both on TiO_2 (P-25) and impregnated V/TiO_2 (Fig. 4A and B). The time course results were quantitatively the same on the two catalysts. Negligible carbon dioxide and water (at 5 h) formations were observed on impregnated V/TiO_2 and TiO_2 (P-25), respectively. As mentioned above under UV–vis light (Fig. 2B), the apparent increase of ethanol in first 1 h may be the contribution of produced formic acid [34].

In summary, under the illumination of visible light only, the ethanol dehydration rates followed the order (Table 1B)

$$\text{mesoporous V}-\text{TiO}_2 > \text{V/mesoporous TiO}_2 \gg \text{mesoporous TiO}_2 > \text{TiO}_2 > \text{V/TiO}_2 \quad (4)$$

Ethanol dehydrogenation rates followed the order

$$\text{V/TiO}_2 > \text{TiO}_2 \gg \text{mesoporous V}-\text{TiO}_2 > \text{mesoporous TiO}_2 \approx \text{V/mesoporous} - \text{TiO}_2 \quad (5)$$

No acetic acid and negligible carbon dioxide were formed on all V + TiO_2 catalysts under the illumination of visible light only. Under dark conditions at room temperature, no reaction proceeded in ethanol and O_2 over Pt-doped TiO_2 catalyst [7].

3.3. Diffuse-reflectance UV–vis absorption spectra for V–TiO_2 catalysts

UV–vis spectra were measured for V + TiO_2 catalysts in diffuse-reflectance mode. In comparison to the absorption data for TiO_2 (P-25), the absorption was extended to the higher

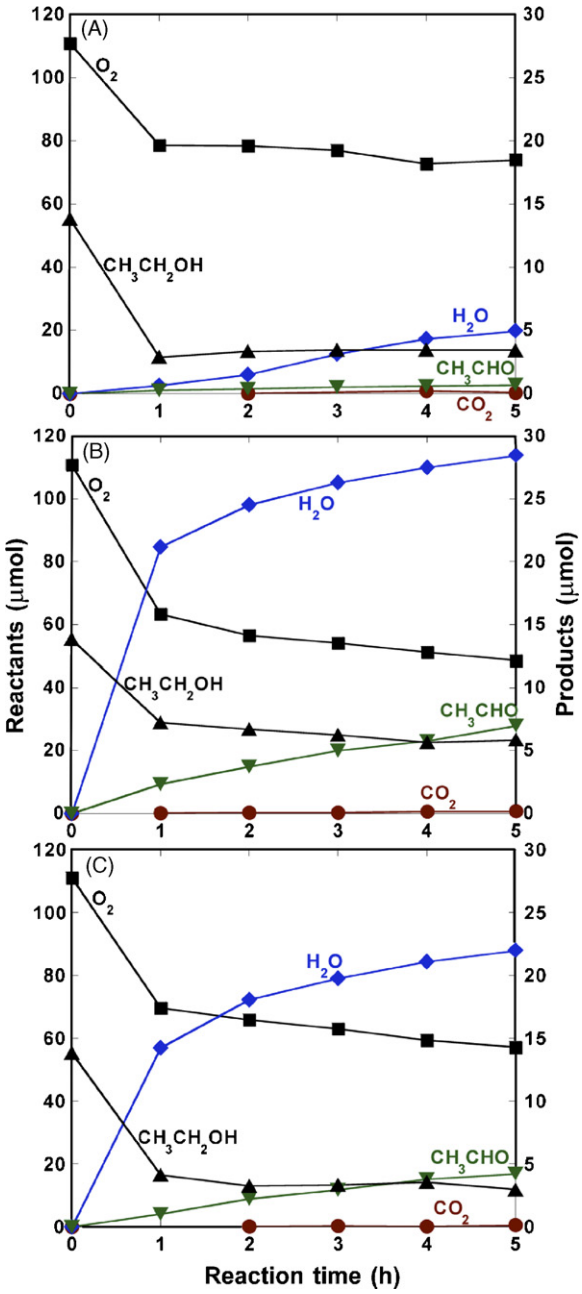

Fig. 3. Ethanol oxidation reaction as a function of time under the illumination of visible light only on mesoporous V + TiO_2 catalysts. Reaction conditions were the same as noted in the caption for Fig. 1. (A) Mesoporous TiO_2. (B) Mesoporous V–TiO_2 (3.0 wt% V). (C) Impregnated V/mesoporous TiO_2 (3.0 wt% V).

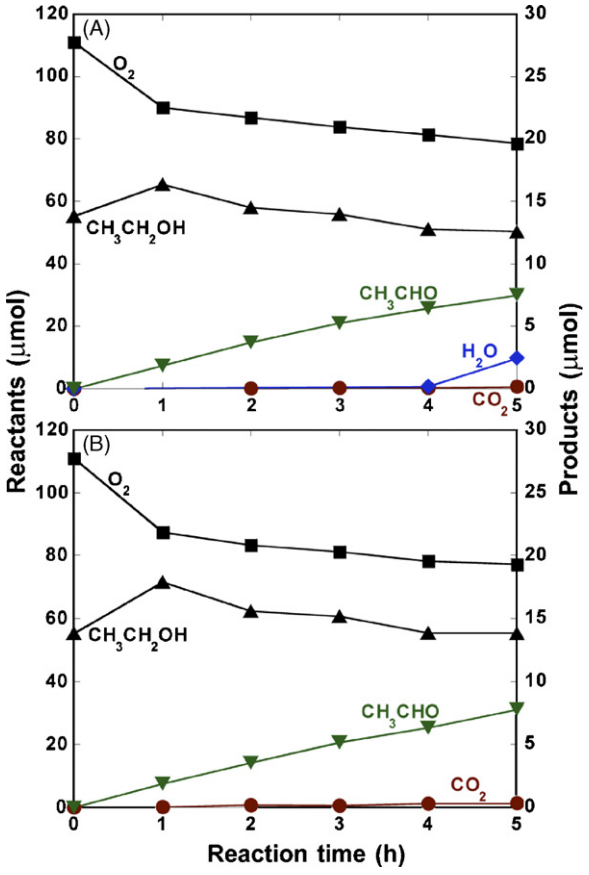

Fig. 4. Ethanol oxidation reaction as a function of time under the illumination of visible light only on conventional V + TiO_2 (P-25) catalysts. Reaction conditions were the same as noted in the caption for Fig. 1. (A) TiO_2 (P-25). (B) Impregnated V/TiO_2 (3.0 wt% V).

wavelength side when 1.0–3.0 wt% of V was impregnated (Fig. 5a–c) [4,8]. The extension toward visible light side was more enhanced for mesoporous TiO_2-based catalysts. Similar to the vanadium impregnation with TiO_2 (P-25), the V impregnation with mesoporous TiO_2 progressively extended the light absorption toward visible light region (Fig. 5g and h). In contrast, the extent of extension was independent to the V contents in catalysts for mesoporous V–TiO_2 between 1.0 and 3.0 wt% of V (Fig. 5e and f, respectively). The extent of extension toward visible light region was in the order

$$\begin{aligned}&\mathrm{V/mesoporous\ TiO_2}(3.0\%) > \mathrm{mesoporous\ V}\\&\quad -\mathrm{TiO_2}(1.0-3.0\%) > \mathrm{V/mesoporous\ TiO_2}(1.0\%)\\&\quad > \mathrm{V/TiO_2}(3.0\%) > \mathrm{mesoporous\ TiO_2} > \mathrm{V/TiO_2}(1.0\%)\\&\quad > \mathrm{TiO_2\ (P\text{-}25)}\end{aligned} \tag{6}$$

4. Discussion

Under the illumination of UV + visible light, total formation rates on carbon basis were in the order (Table 1)

$$\begin{aligned}&\mathrm{mesoporous\ TiO_2} > \mathrm{mesoporous\ V{-}TiO_2} > \mathrm{TiO_2} >\\&\quad \mathrm{V/mesoporous\ TiO_2} > \mathrm{V/TiO_2}\end{aligned} \tag{7}$$

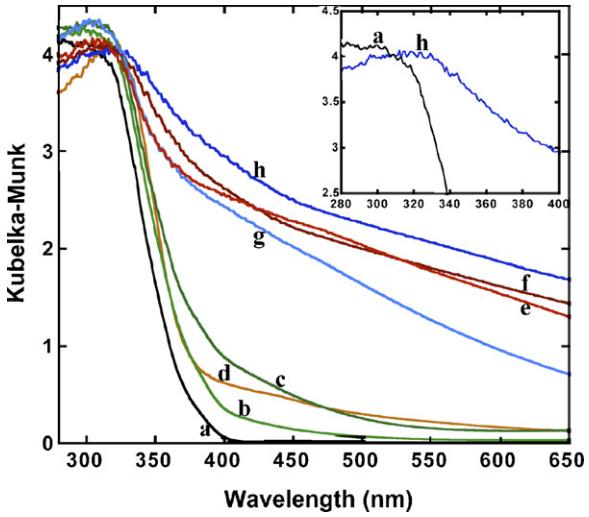

Fig. 5. Diffuse-reflectance UV–vis absorption spectra for TiO_2 (P-25) (a), impregnated V/TiO_2 (P-25) (1.0 and 3.0 wt% V) (b and c, respectively), mesoporous TiO_2 (d), mesoporous V–TiO_2 (1.0 and 3.0 wt% V) (e and f, respectively), and impregnated V/mesoporous TiO_2 (1.0 and 3.0 wt% V) (g and h, respectively). (Inset) Expanded data in the region between 280 and 400 nm for TiO_2 (P-25) (a) and V/mesoporous TiO_2 (3.0 wt% V) (h).

As a general trend, mesoporous TiO_2-based catalysts were superior to anatase TiO_2-based catalysts (Table 1A). Various kinds of specific photocatalysis under the illumination of light > 320 nm was reported using mesoporous TiO_2 [35]. Acetic acid that was further oxidized from acetaldehyde was exclusively found in the mesoporous TiO_2-based catalysis. The doping of vanadium did not always work positively. Typical trend by the doping of vanadium cannot be found either in mesoporous (amorphous) TiO_2 or anatase TiO_2.

Under the illumination of *visible light only*, total formation rates on carbon basis followed the order (Table 1B)

$$\begin{aligned}&\mathrm{mesoporous\ V{-}TiO_2} > \mathrm{TiO_2} \approx \mathrm{V/TiO_2}\\&\quad > \mathrm{V/mesoporous\ TiO_2} \gg \mathrm{mesoporous\ TiO_2}\end{aligned} \tag{8}$$

Only mesoporous V–TiO_2 was superior to anatase TiO_2-based catalysts. Other mesoporous TiO_2-based catalysts were even worse than anatase TiO_2-based ones. Two groups of V + TiO_2 catalysts showed clear contrast. Ethanol dehydration proceeded on mesoporous TiO_2-based catalysts whereas exclusive dehydrogenation proceeded on anatase-TiO_2 based catalysts. For the 2-propanol decomposition, product switching from acetone (dehydrogenation) to propene (dehydration) was reported as the increase of vanadium content in V/TiO_2(anatase) catalysts at 473 K [36].

It is contradictory that the initial water formations on mesoporous V–TiO_2 and V/mesoporous TiO_2 were even faster when illuminated with visible light only than under the illumination both UV and visible light (Table 1). This may be rationalized by assuming the balance between acetaldehyde/acetic acid desorption and further consecutive oxidation reaction steps finally to form H_2O and CO_2, CO, or

carbonaceous species adsorbed

$$C_2H_5OH + (x+1)O_2 \rightarrow 3H_2O + 2CO_x \quad (x = 2, 1, \text{or} 0) \tag{9}$$

The consumption rates ratio of O_2 and ethanol in the first 1 h were 1.8 and 1.1 for mesoporous V–TiO_2 and V/mesoporous TiO_2, respectively (Fig. 3B and C). In addition to constant dehydration reaction to form acetaldehyde and water, further breakdown reaction(s) via equation (9) may have proceeded in first 1 h on the two mesoporous TiO_2-based catalysts to form CO_2 and/or carbonaceous species (Table 1B). When water was mixed in the reactants ethanol and O_2 for the photo-oxidation reaction on Pd- and Cu-modified TiO_2(anatase) catalysts, catalytic formation of acetaldehyde was active and constant along with the minor formation of ethyleneglycol [33]. On the other hand, photocatalytic activity of pure TiO_2(anatase) and one doped with Fe became deactivated during the time course [33]. Thus, the possibility cannot be excluded in this study that initially formed water modified the mesoporous V + TiO_2 catalysts in Fig. 3B and C within 1 h of reaction.

The effects of vanadium doping were remarkable in mesoporous TiO_2-based catalysts whereas no effects of V doping were detected in anatase TiO_2-based catalysts (Table 1B).

The vanadium local structure was reported for these V + TiO_2 catalysts [29]. Common vanadium(V) surface dispersed species (Fig. 6A) [25,27,29] was suggested for impregnated V/mesoporous TiO_2, impregnated V/TiO_2 (P-25), and sol–gel V–TiO_2 whereas V(IV) sites substituted on the Ti sites of mesoporous TiO_2 matrix for mesoporous V–TiO_2 (Fig. 6B). The relevance to ethanol photo-oxidation is first considered for data with the illumination of UV + visible light listed in Table 1A. The phase of support TiO_2, amorphous (mesoporous) or predominant anatase (P-25), was the primary factor to control the catalysis. The doping of V(V) deactivated the catalysis to form acetaldehyde, water, or acetic acid in both environments [V/mesoporous TiO_2 and V/TiO_2 (P-25)]. The doping of V(IV) maintained the total activity of mesoporous TiO_2 and directed the formation of acetic acid rather than predominant acetaldehyde over mesoporous V–TiO_2 (Fig. 6B and Table 1A). The photocatalytic activity of sol–gel V–TiO_2 catalysts in which V(IV) sites substituted on the Ti sites of TiO_2 was reported for the decompositions of methylene blue and acetaldehyde either under UV light or under visible light [6].

For the ethanol photo-oxidation with the illumination of visible light only, the phase of TiO_2 primarily controlled the catalysis again (Table 1B). The doping of both V(IV) and V(V) promoted the catalysis, however, only to mesoporous TiO_2. The total formation rates increased more by the doping of V(IV) (9.2 times, mesoporous V–TiO_2) than by V(V) doping (4.4 times, V/mesoporous TiO_2). These catalytic trends were consistent with extension of optical absorption spectra toward visible light wavelength region for mesoporous V–TiO_2 and V/mesoporous TiO_2 (Fig. 5).

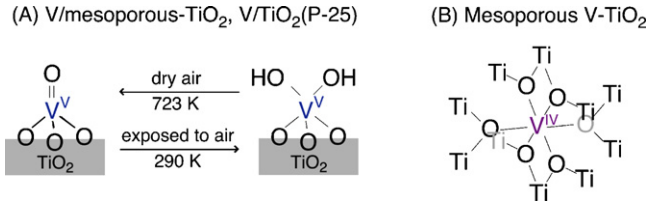

Fig. 6. Vanadium site models suggested by V K-edge XAFS study common for V/mesoporous TiO_2 and impregnated V/TiO_2 (P-25) (A) and for mesoporous V–TiO_2 (B).

5. Conclusions

(1) Under the illumination of UV + visible light, mesoporous V + TiO_2 catalysts generally showed faster ethanol oxidation reaction than anatase V + TiO_2 catalysts did. Major products were acetaldehyde, water, acetic acid, and carbon dioxide. Deeply oxidized acetic acid and carbon dioxide were preferably formed over the mesoporous V + TiO_2 catalysts.

(2) Under the illumination of visible light only, mesoporous V–TiO_2 catalyst was best and superior to anatase V + TiO_2 catalysts. The phase of TiO_2 controlled the product selectivity. Ethanol dehydration and dehydrogenation proceeded on mesoporous V + TiO_2 and V + TiO_2(anatase) catalysts, respectively. V^{IV} doping was effective than V^{V} doping to mesoporous TiO_2, however, vanadium had no effects to anatase TiO_2.

(3) Initial water evolution from mesoporous V–TiO_2 and V/mesoporous TiO_2 catalysts under the illumination of visible light only suggested specific catalysis utilizing the mesopore environment. Consecutive oxidation reactions to H_2O and CO_x ($x = 0$, 1, and 2) were suggested.

(4) The improved photo-oxidation performance of mesoporous V–TiO_2 (and V/mesoporous TiO_2) catalyst(s) was correlated with the extension of optical absorption spectra toward visible light wavelength region.

Acknowledgements

The authors are thankful for financial support from the Grant-in-Aid for Scientific Research (YI, C-17550073, B-13555230) and that on the Priority Area "Molecular Nanodynamics" (YI, 432-17034013) from the Ministry of Education, Culture, Sports, Science, and Technology of Japan. The XAFS experiments were performed under the approval of the SPring-8 Program Review Committee (2003A0146-NX-np and 2002B0739-NX-np) and that of the Photon Factory Proposal Review Committee (2001G308 and 2002G285).

References

[1] P. Pichat, in: G. Ertl, H. Knözinger, J. Weitkamp (Eds.), Handbook of Heterogeneous Catalysis, vol. 4, VCH, Weinheim, 1997, pp. 2111–2122.
[2] A. Fujishima, T.N. Rao, D.A. Tryk, J. Photochem. Photobiol. C Photochem. Rev. 1 (2000) 1–21.
[3] M. Anpo, Bull. Chem. Soc. Jpn. 77 (2004) 1427–1442.
[4] S.T. Martin, C.L. Morrison, M.R. Hoffmann, J. Phys. Chem. 98 (1994) 13695–13704.

[5] M. Anpo, M. Takeuchi, J. Catal. 216 (2003) 505–516.
[6] K. Iketani, R.D. Sun, M. Toki, K. Hirota, O. Yamaguchi, Mater. Sci. Eng. B 108 (2004) 187–193.
[7] A.V. Vorontsov, V.P. Dubovitskaya, J. Catal. 221 (2004) 102–109.
[8] J.C.S. Wu, C.H. Chen, J. Photochem. Photobiol. A Chem. 163 (2004) 509–515.
[9] M. Sathish, B. Viswanathan, R.P. Viswanath, C.S. Gopinath, Chem. Mater. 17 (2005) 6349–6353.
[10] J.C. D'Oliveira, C. Guillard, C. Millarad, P. Pichat, J. Environ. Sci. Health A 28 (1993) 941–962.
[11] G.K.C. Low, S.R. McEvoy, R.W. Matthews, Environ. Sci. Technol. 25 (1991) 460–467.
[12] D.F. Ollis, Environ. Sci. Technol. 19 (1985) 480–484.
[13] J.C. D'Oliveira, W.D.W. Jayatilake, K. Tennakone, J.M. Herrmann, P. Pichat, in: D.E. Ollis, H. Al-Ekabi (Eds.), Photocatalytic Purification and Treatment of Water and Air, Elsevier, Amsterdam, 1993, pp. 601–606.
[14] Q. Dai, N. He, Y. Guo, C. Yuan, Chem. Lett. (1998) 1113–1114.
[15] B. Smarsly, D. Grosso, T. Brezesinski, N. Pinna, C. Boissiere, M. Antonietti, C. Sanchez, Chem. Mater. 16 (2004) 2948–2952.
[16] F. Schuth, Chem. Mater. 13 (2001) 3184–3195.
[17] Y. Wang, X. Tang, L. Yin, W. Huang, Y.R. Hacohen, A. Gedanken, Adv. Mater. 12 (2000) 1183–1186.
[18] Y. Yue, Z. Gao, Chem. Commun. (2000) 1755–1756.
[19] Y. Wang, C. Ma, X. Sun, H. Li, J. Non-Cryst. Solids 319 (2003) 109–116.
[20] T.Z. Ren, Z.Y. Yuan, B.L. Su, Colloids Surf. A Physicochem. Eng. Aspects 241 (2004) 67–73.
[21] D. Zhang, L. Qi, Chem. Commun. (2005) 2735–2737.
[22] K. Liu, M. Zhang, K. Shi, H. Fu, Mater. Lett. 59 (2005) 3308–3310.
[23] H. Yoshitake, T. Sugihara, T. Tatsumi, Chem. Mater. 14 (2002) 1023–1029.
[24] H. Yoshitake, T. Tatsumi, Chem. Mater. 15 (2003) 1695–1702.
[25] B. Olthof, A. Khodakov, A.T. Bell, E. Iglesia, J. Phys. Chem. B 104 (2000) 1516–1528.
[26] J. Haber, A. Kozlowska, R. Kozlowski, J. Catal. 102 (1986) 52–63.
[27] G. Deo, I.E. Wachs, J. Phys. Chem. 95 (1991) 5889–5895.
[28] A. Vejux, P. Courtine, J. Solid State Chem. 23 (1978) 93–103.
[29] Y. Izumi, F. Kiyotaki, N. Yagi, A.M. Vlaicu, A. Nisawa, S. Fukushima, H. Yoshitake, Y. Iwasawa, J. Phys. Chem. B 109 (2005) 14884–14891.
[30] S.J. Hwang, D. Raftery, Catal. Today 49 (1999) 353–361.
[31] D.V. Kozlov, E.A. Paukshtis, E.N. Savinov, Appl. Catal. B Environ. 24 (2000) L7–L12.
[32] E. Piera, J.A. Ayllon, X. Domenech, J. Peral, Catal. Today 76 (2002) 259–270.
[33] J. Arana, J.M.D. Rodriguez, O.G. Diaz, E.T. Rendon, J.A.H. Helian, G. Colon, J.A. Navio, J.P. Pena, J. Mol. Catal. A Chem. 215 (2004) 153–160.
[34] S. Klosek, D. Reftery, J. Phys. Chem. B 105 (2001) 2815–2819.
[35] Y. Shiraishi, N. Saito, T. Hirai, J. Am. Chem. Soc. 127 (2005) 12820–12822.
[36] M. Gasior, I. Gasior, B. Grzybowska, Appl. Catal. 10 (1984) 87–100.